Marine Geophysical Researches 22: 265-287, 2001.

Velocity-Interface Structure of the Southwestern Ryukyu Subduction Zone from EW9509-1 OBS/MCS Data

Tan K. Wang[1,*], Kirk McIntosh[2], Yosio Nakamura[2], Char-Shine *Liu*[3] and How-Wei Chen[4]

[1]*Institute of Applied Geophysics, National Taiwan Ocean University, Keelung, Taiwan, ROC;*

[2]*Institute for Geophysics, University of Texas, Austin, Texas, USA;*

[3]*1nstitute of Oceanography, National Taiwan University, Taipei, Taiwan, ROC;*

[4]*Institute of Applied Geophysics, National Chung Cheng University, Chiayi, Taiwan, ROC;*

[*]*Author for correspondence (Fax: 886-2-24625038; E-mail: tkwang@mail.ntou.edu.tw)*

Key words: **OBS, crustal structure, subduction, ray, travel-time**

Abstract

A wide-angle seismic survey, combining ocean-bottom seismometers (OBS) and multi-channel seismic (MCS) profiling, was implemented in the southwestern Ryukyu subduction zone during August and September 1995. In this paper, we present the data analysis of eight OBSs and the corresponding MCS line along profile EW9509-1 from this experiment. Seismic data modeling includes identification of refracted and reflected arrivals, initial model building from velocity analysis of the MCS data, and simultaneous and layer-stripping inversions of the OBS and MCS arrivals. The velocity-interface structure constructed along profile EW9509-1 shows that the northward subduction of the Philippine Sea Plate has resulted in a northward thickening of the sediments of the Ryukyu Trench and the Yaeyama accretionary wedge north of the trench. The boundary between the subducting oceanic crust and the overriding continental crust (represented by a velocity contour of 6.75 km/s) and a sudden increase of the subducting angle (from 5 degrees to 25 degrees) are well imaged below the Nanao Basin. Furthermore, velocity undulation and interface variation are found within the upper crust of the Ryukyu Arc. Therefore, the strongest compression due to subduction and a break-off of the slab may have occurred and induced the high seismicity in the forearc region.

Introduction

Crustal structures imaged by ocean-bottom seismometer (OBS) data using air-gun sources generally fill gaps between shallow structures obtained from multichannel seismic (MCS) profiles and deeper structures obtained using earthquake seismology in the marine environment. Several OBS surveys in the northeastern, middle and southwestern Ryukyu subduction zones were successfully implemented for imaging of the crustal structures in 1984, 1988 and 1985/1995, respectively (Figure 1). An OBS velocity model of 1984-2 (Iwasaki et al., 1990) shows that the subducting angle changes from about 5 degrees to 10 degrees below the southeastern part of the sedimentary wedge in the northeastern Rvukvu subduction zone. It was also found that the continental crust at the collision front is deformed and dragged down by subduction of the oceanic crust. On the other hand, the subducting angle in an OBS velocity model of 1988-2A in the middle Ryukyu subduction zone is uniform and about 5 degrees (Kodaira et al., 1996). The first OBS survey in the southwestern subduction zone was conducted in 1985 by Hagen et al. (1988). Their results illustrated the northward subduction of the PSP beneath the Ryukyu Arc but were not well constrained in the lower crust. Although OBS data acquired in the Ryukyu Arc have provided reliable P-wave velocity models of the crustal structures, the intra-crustal interfaces and the sedimentary structures could not be well imaged due to weak air-gun shots, insufficient trace spacing and a lack of combined MCS data in the experiments.

Using a large air-gun array and incorporating MCS data, three profiles of the OBS data (EW9509-14, EW9509-16 and EW9509-23) were acquired in the southwestern Ryukyu subduction zone (Figure 1). An OBS velocity model of EW9509-14 (McIntosh and Nakamura, 1998) shows that the thickness of the Ryukyu Arc basement (velocity > 5 km/s) and the subducting Philippine Sea Plate (PSP) below the Nanao Basin (intersection with EW9509-1) are 10-12 km and 8-12 km, respectively. Results from modeling the OBS data of profile EW9509-16 (Wang and Chiang, 1998) suggest that the thickness of the Ryukyu Arc basement (5.5-6.75 km/s) and the subducting PSP crust (6.75-7.75 km/s) are 10-15 km and 8-12 km, respectively. An OBS velocity model of EW9509-23 (Yang and Wang, 1998) off southeastern Taiwan shows that the thickness of the oceanic crust (4.5-7.75 km/s) southeast of OBS station 31 is 5-7 km. Northwest of OBS station 31, the crust thickens northwestward.

The previous results of OBS data modeling in the Ryukyu subduction zone have lacked sufficient constraints on the structural interfaces from the reflected arrivals of seismic data. In this paper, we present travel-time modeling (Zelt, 1999) of an EW9509-1 MCS/OBS profile parallel to the subduction direction. This modeling approach includes identification of refracted and reflected arrivals, velocity analysis of the MCS data, simultaneous inversion of MCS arrivals and the individual phase in the OBS data, and minimum parameterization of the model grids.

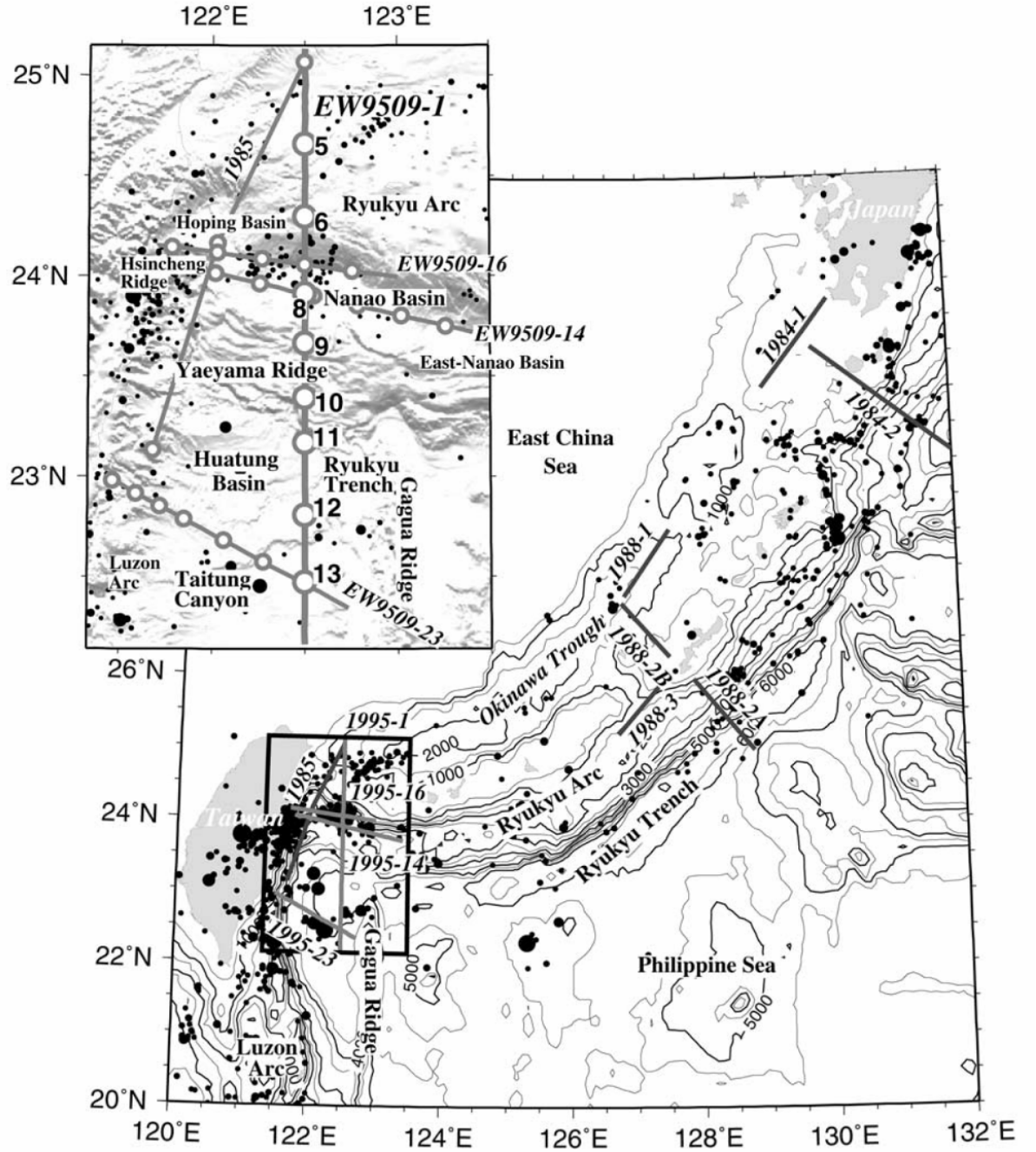

Figure 1. OBS lines, teleseismically determined epicenters (CNSS catalogue), bathymetry and tectonic features in the Ryukyu subduction zone. Two OBS surveys of the southwestern Ryukyu Arc was conducted in 1985 and 1995 within the area inside the black frame, enlarged in the illuminated bathymetry (Liu et al., 1998) in the upper left corner. Other OBS experiments in the middle (Kodaira et al., 1996) and northeastern (Iwasaki et al., 1990) Ryukyu Arcs are denoted by the years, 1988 and 1984, respectively, in which they were conducted. The contour interval of bathymetry is 500 m. In the inset, the OBS stations and the OBS/MCS lines are indicated by open circles and solid lines, respectively. In particular, only the EW9509-1 seismic line (thicker) with eight OBSs (open circles) is investigated in this study.

Table 1. OBS locations, maximum offsets and number of traces.

OBS station	OBS 13	OBS 12	OBS 11	OBS 10	OBS 9	OBS 8	OBS 6	OBS 5
Longitude (E)	122.49964	122.50081	122.5046	122.50385	122.49992	122.50158	122.49938	122.50127
Latitude (N)	22.47208	22.80522	23.17222	23.39893	23.6695	23.91581	24.29949	24.66324
Depth (m)	4923	5265	5643	4545	2900	3640	293	455
Max. offset[a] (m)	−36680 161211	−73571 156629	−79856 143975	−76665 138467	−79038 125773	−84410 108628	−62002 94710	−62390 54391
No. traces	4742	5611	5723	5716	5724	5711	5054	4019

[a]Negative/positive values indicate the offsets to the south/north

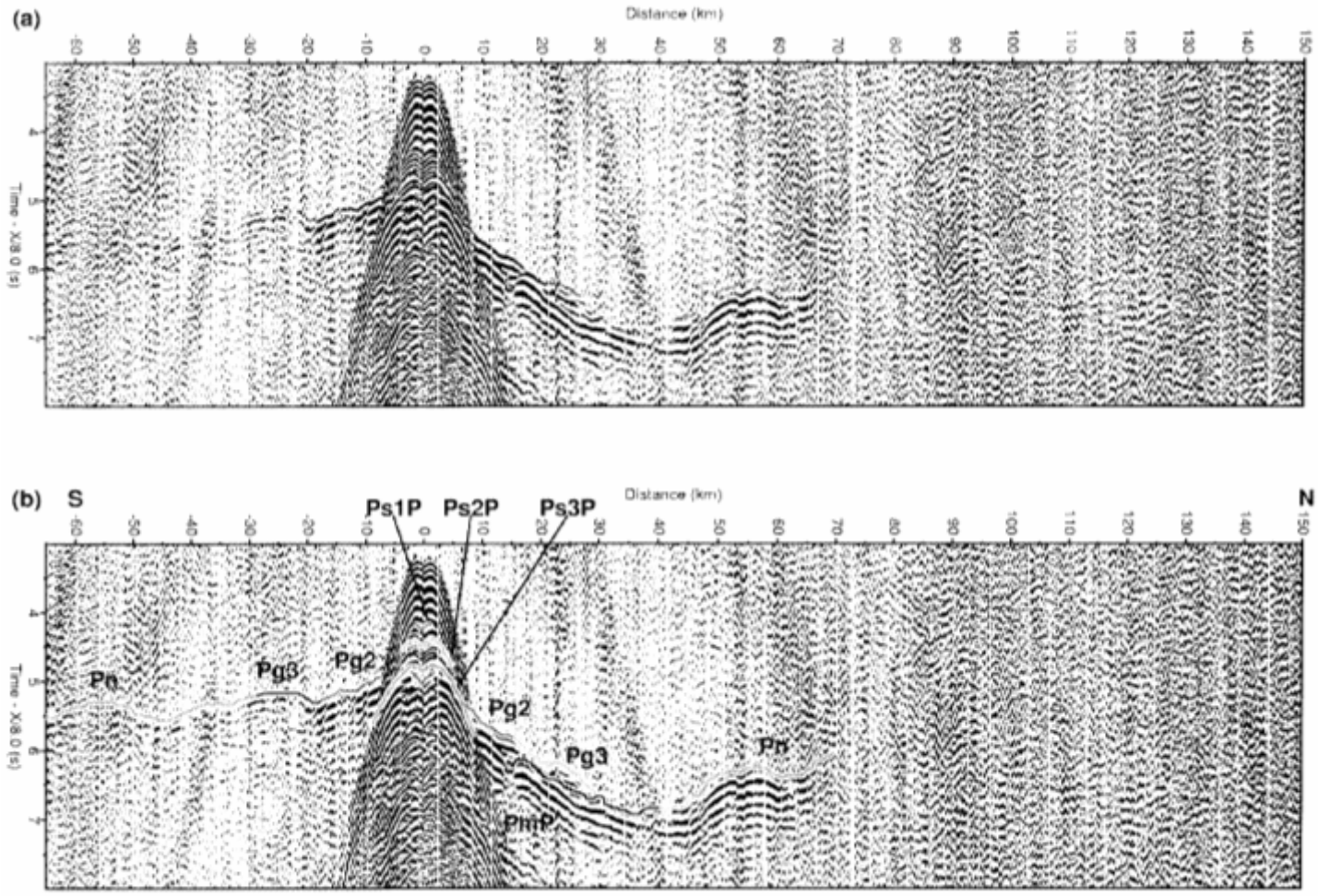

Figure 2. (a) Vertical component of the OBS data and (b) selected arrivals superimposed on the OBS data from station 12 in the Huatung Basin.

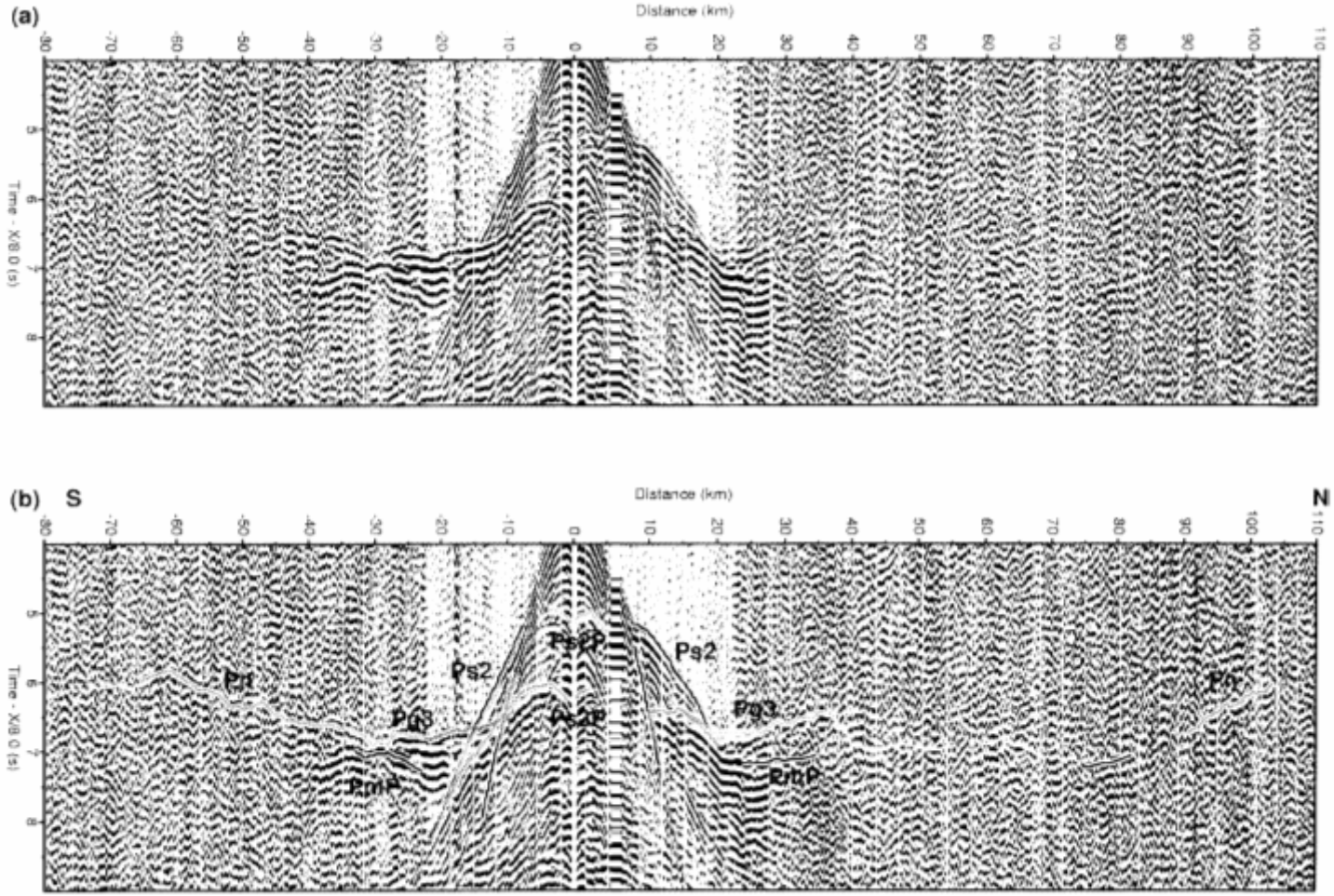

Figure 3. (a) Vertical component of the OBS data and (b) selected arrivals superimposed on the OBS data from station 11 in the Ryukyu Trench. Weak arrivals (white lines) are not used in inversion but are considered to demonstrate the ray coverage shown in Figure 9.

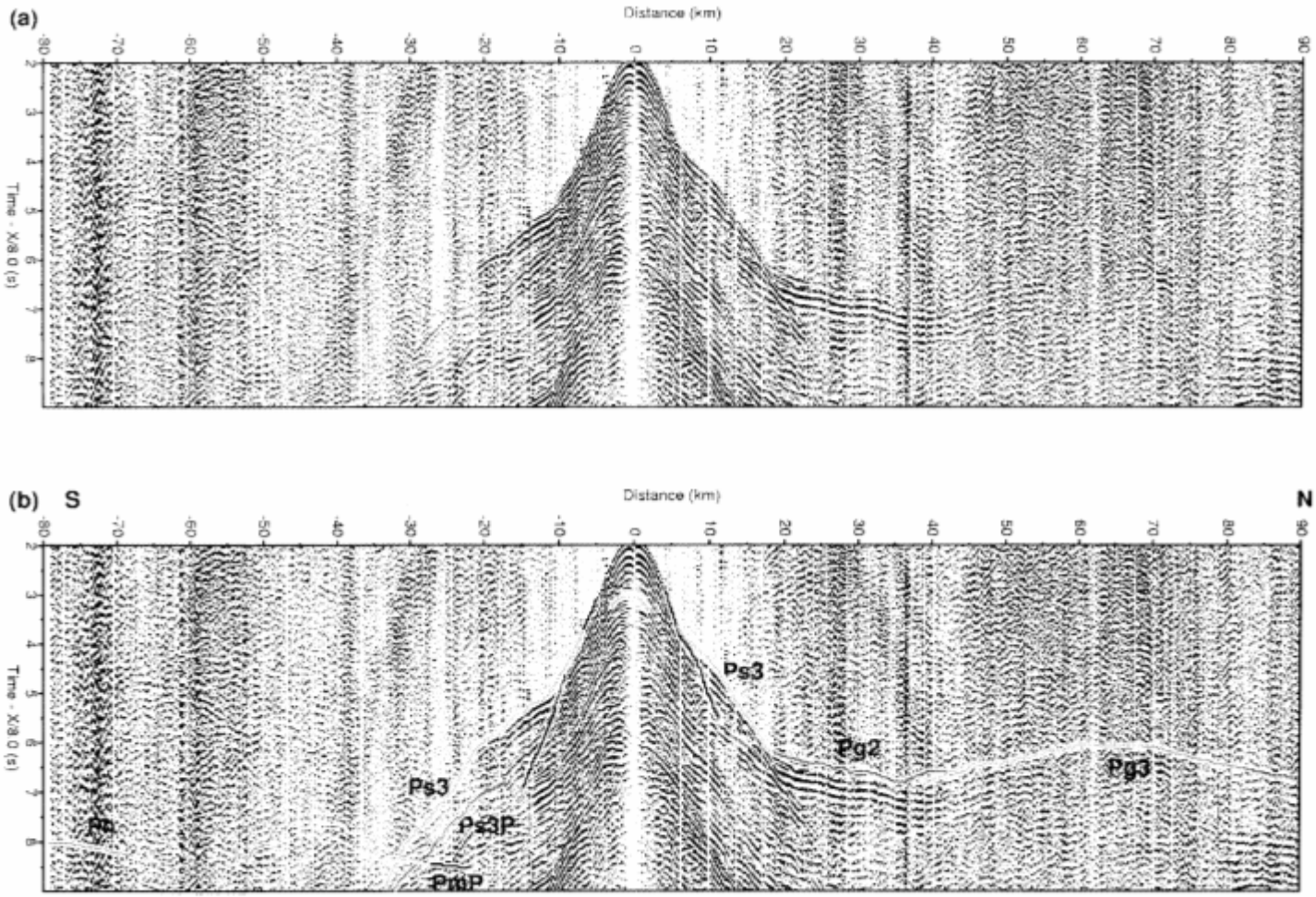

Figure 4. (a) Vertical component of the OBS data and (b) selected arrivals superimposed on the OBS data from station 9 on the northern Yaeyama Ridge. For the first arrivals at the southern far-offset, the upper-mantle refraction (Pn) can be observed, but the refraction through the crust is weak.

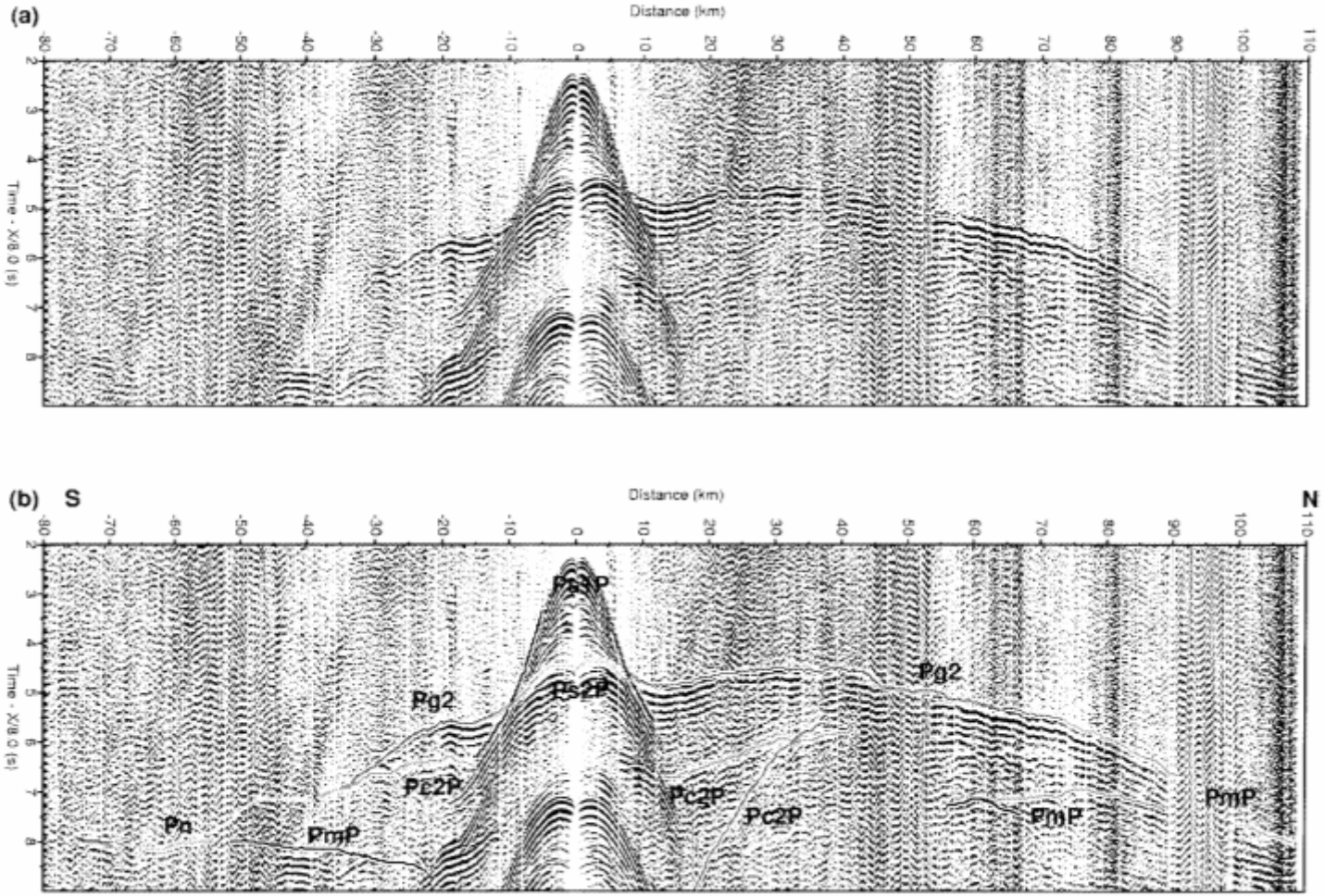

Figure 5. (a) Vertical component of the OBS data and (b) selected arrivals superimposed on the OBS data from station 8 in the Nanao Basin. OBS data of this station demonstrate that the high number of arrival picks may be due to its location in the sedimentary basin and above the thick upper crust where rays travel through more readily.

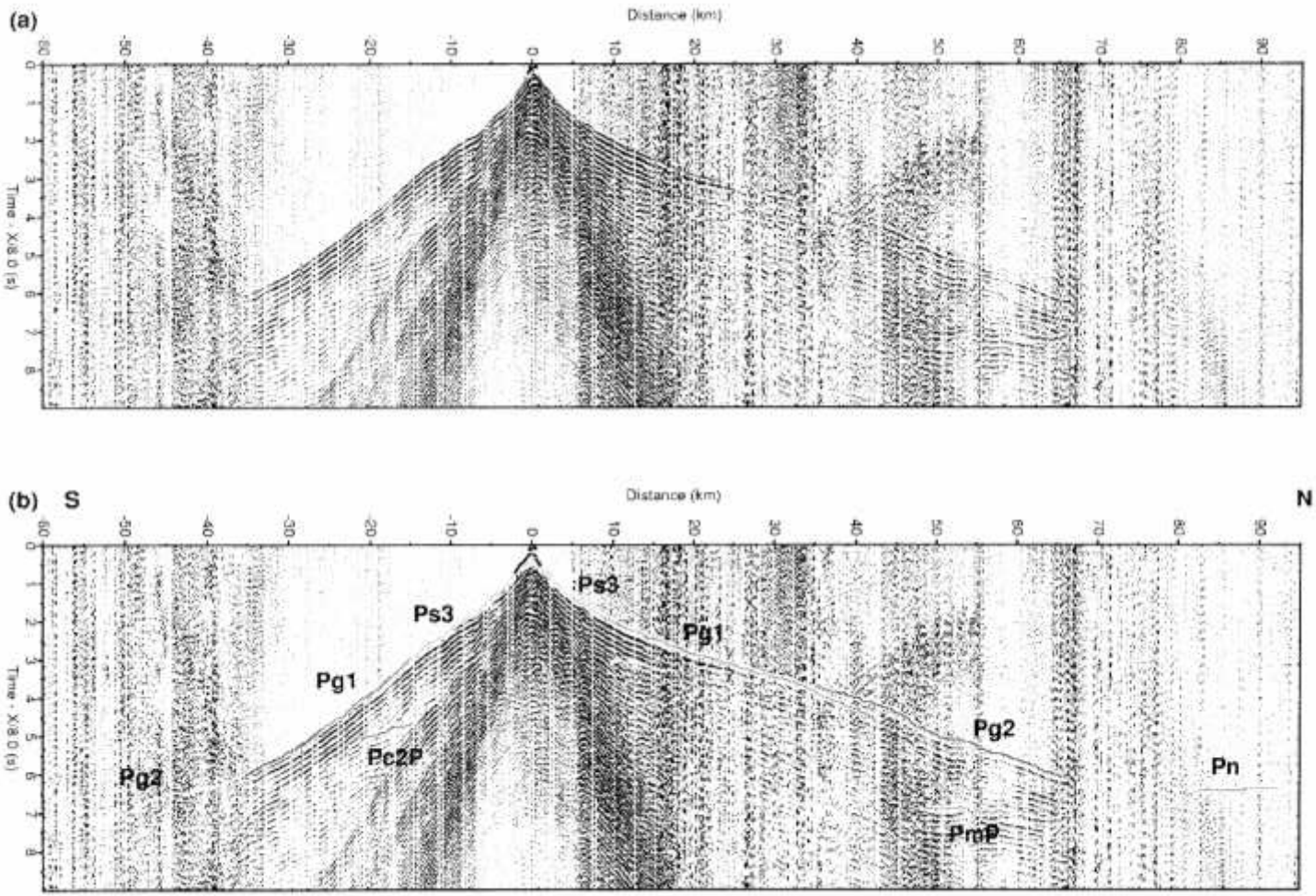

Figure 6. (a) Vertical component of the OBS data and (b) selected arrivals superimposed on the OBS data from station 6 on the top of the Ryukyu Arc slope. (c) Southern far-offset section with weak refracted arrival through the middle crust (Pg2), and (d) northern far-offset section with the refracted arrival through the upper mantle (Pn).

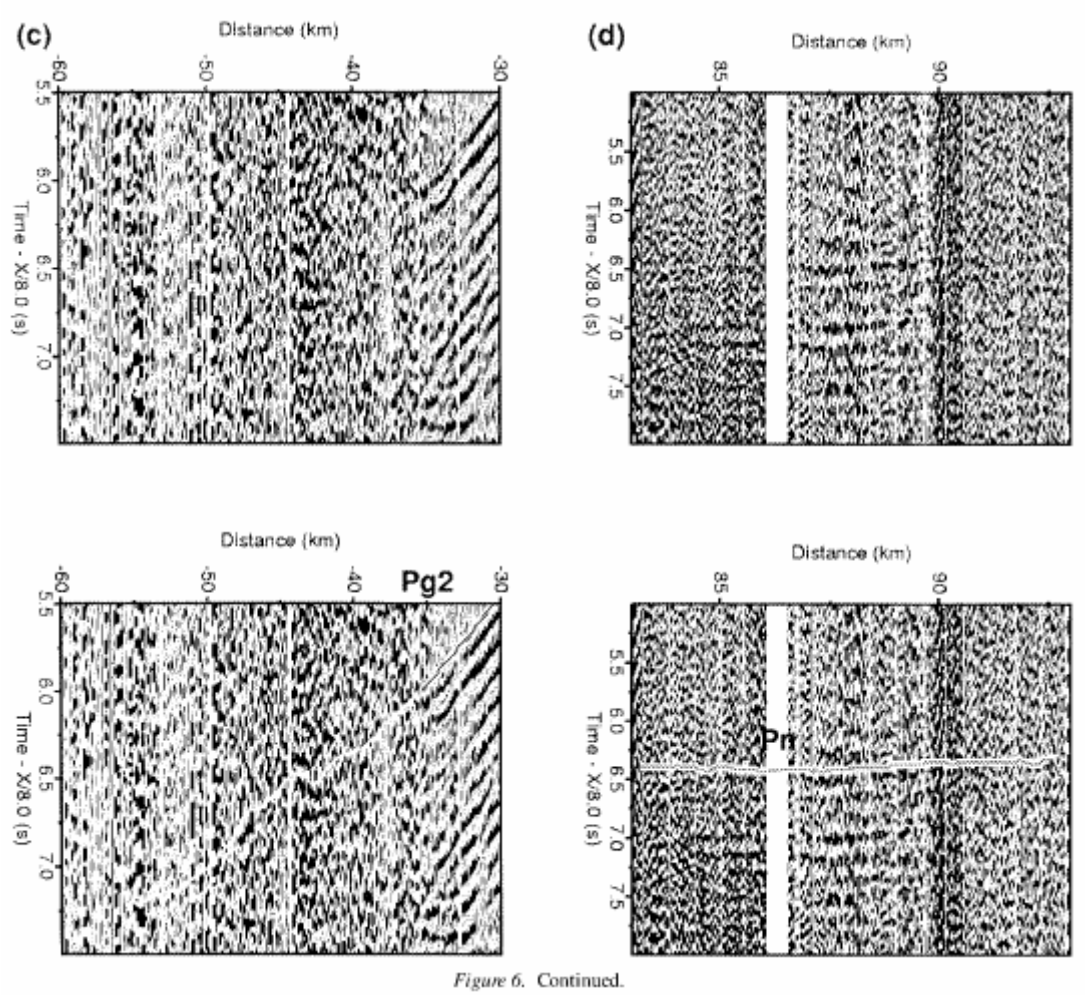

Figure 6. Continued.

Table 2. Nomenclatures of refracted and reflected phases.

	Refractions	Reflections
Upper sediment	Ps1	Ps1P
Lower sediment	Ps2	Ps2P
Compacted sediment	Ps3	Ps3P
Accretionary wedge		
Upper crust	Pg1	Pc1P
Middle crust	Pg2	Pc2P
Lower crust	Pg3	PmP
Upper mantle	Pn	

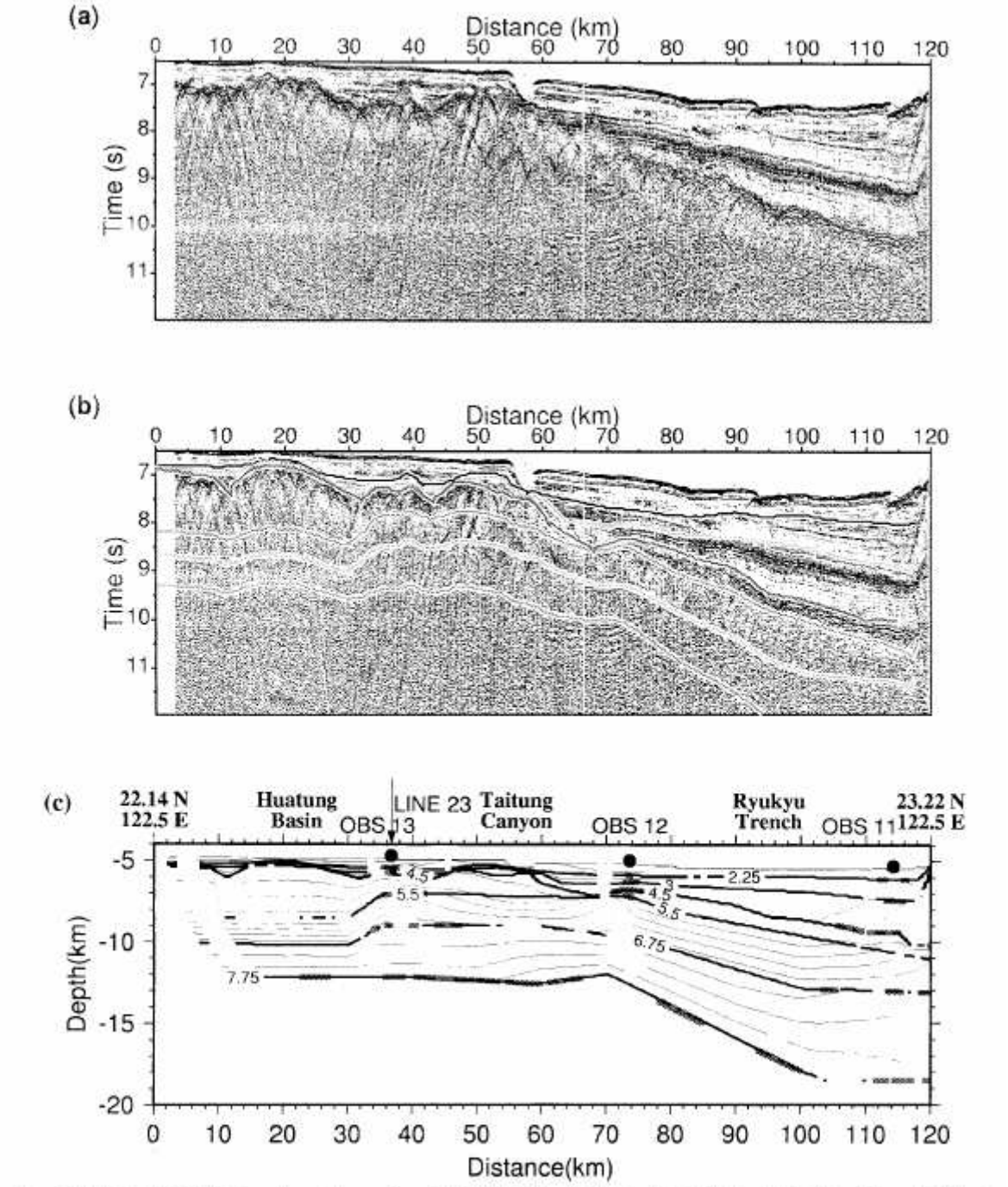

Figure 7. (a) Stacked MCS data along the southern portion of the EW9509-1 (in the Huatung Basin), (b) the calculated travel times (solid lines) superimposed on the stacked section and (c) the associated velocity-interface model developed in this study. The thick lines in (c) are reflection points from OBS data modeling. Velocity contours of 2.25, 3 and 4.5 km/s in (c), which correspond to three sedimentary layers in the Ryukyu Trench and the Huatung Basin, clearly match the reflecting signals in (a). Furthermore, PmP can be identified at least beginning at the Taitung Canyon and extending 15 km northward in (a).

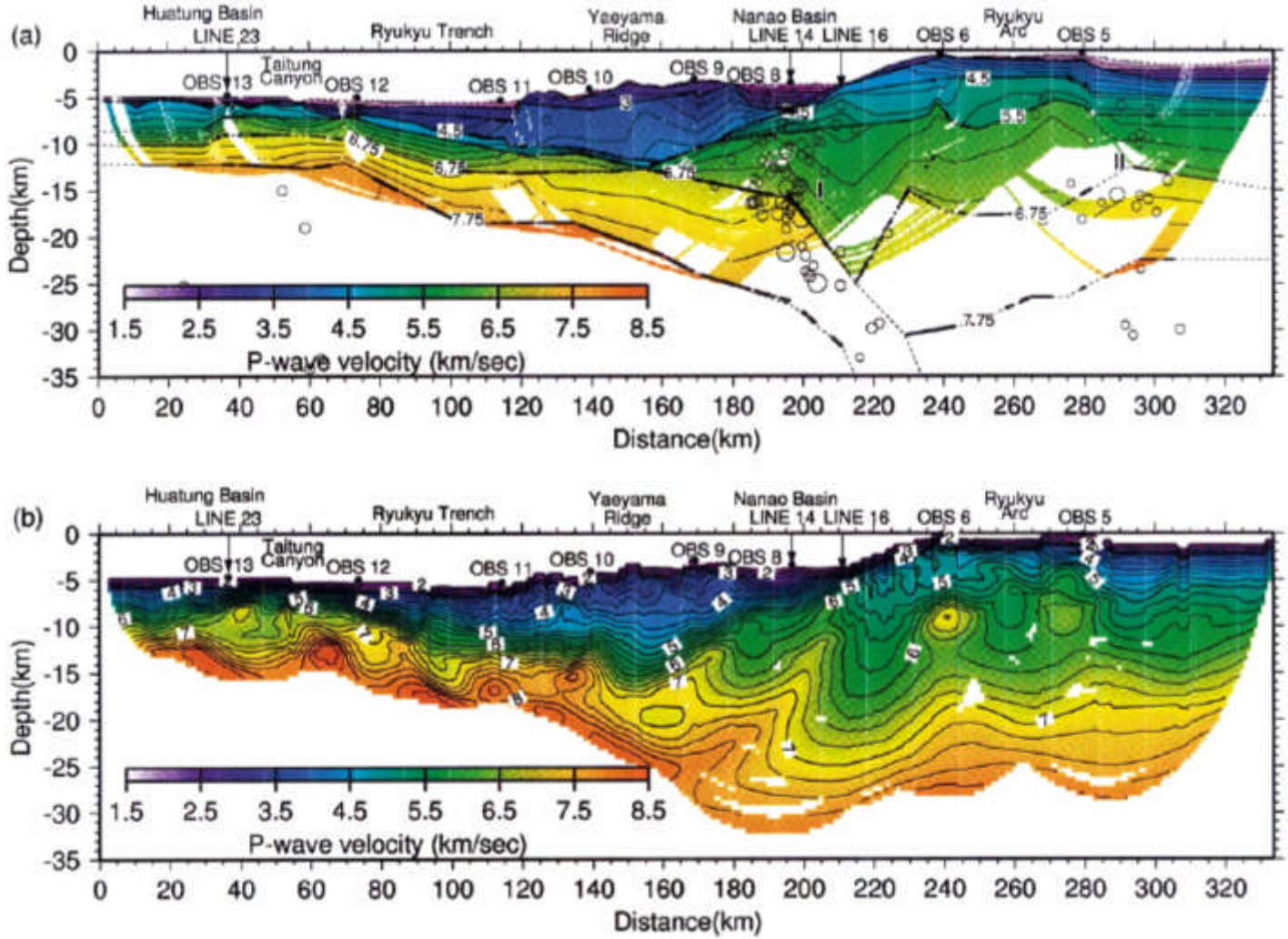

Figure 8. (a) A P-wave velocity-interface model (with coverage of refracted rays associated with apparent arrivals) along profile EW9509-1 in the southwestern Ryukyu subduction zone. The solid black lines are reflection points of the selected arrivals. The open circles are earthquake hypocenters (determined by the Central Weather Bureau, Taiwan) with magnitudes greater than 5, within 40 km of the profile and with errors of the epicenter and the focal depth less than 20 km. (b) A P-wave velocity model of EW9509-1 obtained using non-linear tomography with the refracted arrivals of the OBS data. The contour interval of both models is 0.25 km/s.

Table 3. RMS travel-time residual (ms) for each individual phase and station.

OBS Station	OBS 13		OBS 12		OBS 11		OBS 10		OBS 9		OBS 8		OBS 6		OBS 5	
Location(km)	36.68		73.572		114.199		139.323		169.288		196.568		239.064		279.384	
Offset																
Phase	S	N	S	N	S	N	S	N	S	N	S	N	S	N	S	N
Ps1	50	19	37	65	67	56	44	19	14	64	32	70	X	X	35	60
Ps1P	85	20	36	28	29	17	17	20	36	_	51	38	X	X	60	67
Ps2	_	_	_	_	74	36	78	34	37	_	45	48	30	45	X	X
Ps2P	_	_	12	21	49	28	_	_	38	52	33	34	29	10	X	X
Ps3	_	_	_	_	62	_	55	**90**	**92**	72	62	27	62	52	72	69
Ps3P	50	_	74	52	52	34	52	50	46	_	_	_	_	_	_	_
Pg1	84	_	_	**90**	_	50	58	_	55	X	**92**	69	40	46	61	53
Pc1P	12	46	43	12	_	_	34	18	51	15	42	40	_	_	_	_
Pg2	70	83	77	70	49	59	29	25	32	68	**103**	**91**	**105**	68	87	56
Pc2P	_	40	_	_	_	28	56	25	57	45	29	67	_	_	74	_
Pg3	44	39	63	**94**	86	**102**	47	68	31	55	_	_	**97**	X	89	_	_
PmP	43	55	**96**	**93**	73	71	69	69	76	_	74	**106**	67	_	68	_	_
Pn	19	55	62	87	**158**	88	72	_	89	_	76	X	X	**123**	X	X

'||' marks the boundary of the southern oceanic crust and the northern continental crust. The symbols 'X' and '_' stand for unavailable picks due to pinch-out structures in the model and the weak signals in the OBS data, respectively.

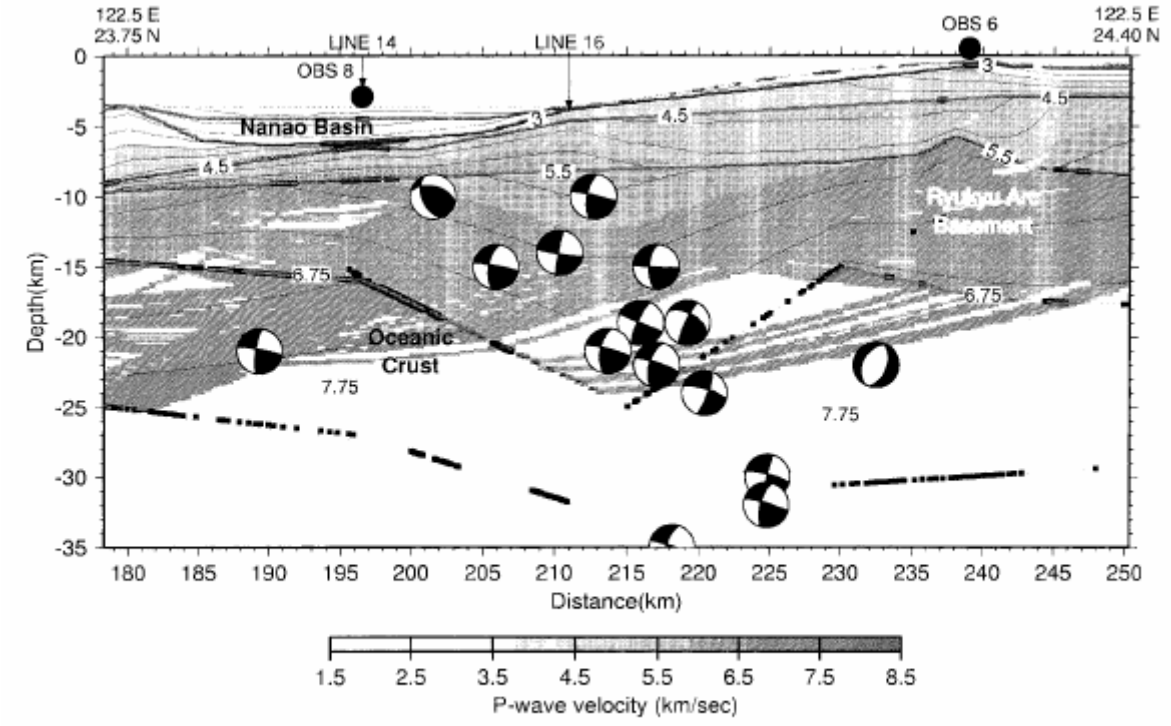

Figure 11. Sedimentary and crustal structures (1:1 scale) of the P-wave velocity and the focal mechanisms (Kao et al., 1998) along profile EW9509-1 in the southwestern Ryukyu forearc region. Focal spheres are projected onto the seismic profile and their darkened quadrants show the first motion of the compressional wave. Errors of the epicenter and the focal depth of these focal mechanisms are generally less than 5 km.

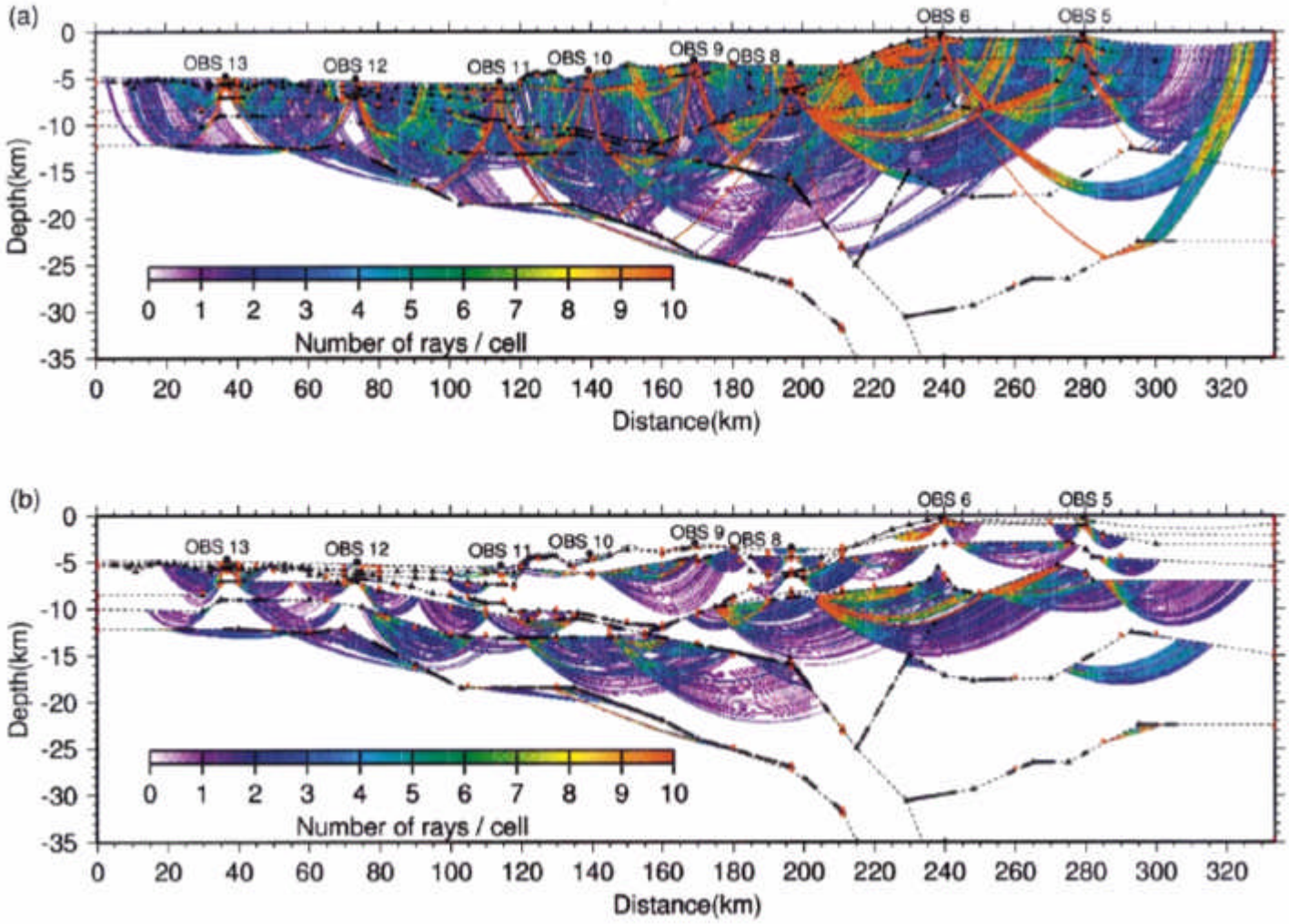

Figure 9. The number of refracted rays in each cell (color shaded) with both apparent and weak arrivals through (a) all layers and (b) their lowest layer along profile EW9509-1. The size of the cell for accounting the number of rays is 0.25 km and 0.05 km along the length and the depth of the model, respectively. Velocity grids (red circles), interface grids (black triangles) and reflection points of the selected arrivals (solid black lines) are also displayed to validate the velocity-interface model.

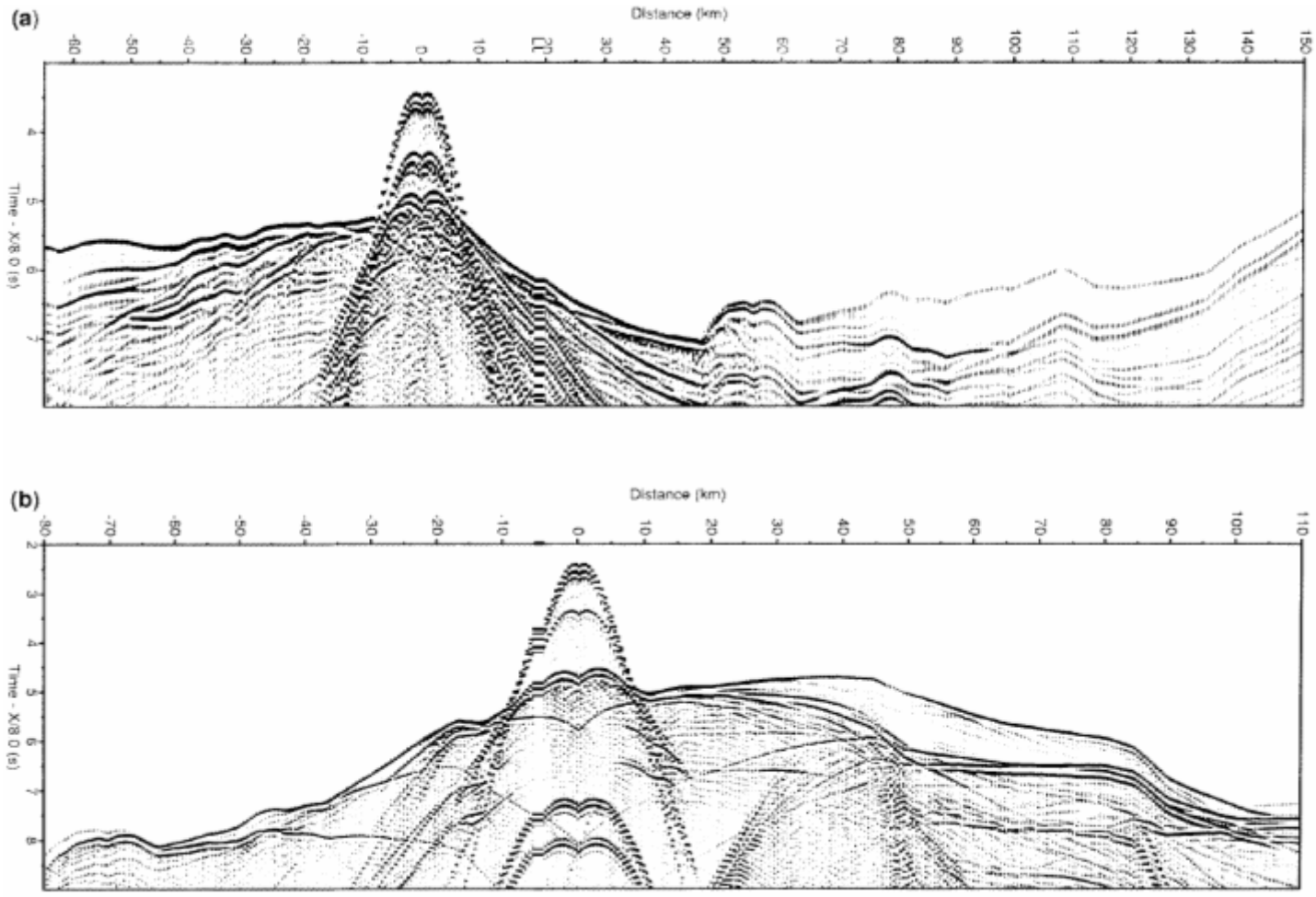

Figure 10. Staggered-grid pseudo-spectral simulation of (a) OBS data from station 12 and (b) OBS data from station 8 in acoustic media.